Iranian Journal of Materials Science and Engineering, Vol. 18, Number 2, June 2021
RESEARCH PAPER

The Effect of Thermal Annealing on Structural, Morphological and Optical Features of $BaTiO_3$ Thin Film Prepared by e-Beam PVD Technique

Namrata Saxena[1], Varshali Sharma[2], Ritu Sharma[1*], Kamlesh Kumar Sharma[1] and Kapil Kumar Jain[3]

***** *rsharma.ece@mnit.ac.in*
[1*] Department of Electronics & Communication, MNIT, Jaipur, India-302017
[2] Department of Electrical and Computer Engineering, Carnegie Mellon University, Pittsburgh, Pennsylvania, United States-15217
[3] Solid State Physics Laboratory, DRDO, New Delhi, India.

Received: July 2020 **Revised: February 2021** **Accepted: April 2021**
DOI: 10.22068/ijmse.1879

Abstract: *The work reported in this paper was focused on the investigation of surface morphological, microstructural, and optical features of polycrystalline $BaTiO_3$ thin film deposited on p-type Si < 100 > substrate using e-beam PVD (physical vapor deposition) technique. The influence of annealing on the surface morphology of the thin film was analyzed by X-ray diffraction, atomic force microscopy and scanning electron microscopy. When the annealing temperature was increased from as-deposited to 800 °C there was a significant growth in the grain size from 28.407 to 37.89 nm. This granular growth of $BaTiO_3$ made the thin film appropriate for nanoelectronic device applications. The roughness of the annealed film was increased from 31.5 to 52.8 nm with the annealing temperature. The optical bandgap was computed using Kubelka-Munk (KM) method which was reduced from 3.93 to 3.87 eV for the as-deposited to the 800 °C annealed film. The above reported properties made the annealed film suitable for optoelectronic applications. For polycrystalline $BaTiO_3$ thin film the refractive index varied from 2.2 to 1.98 from 400 to 500 nm and it was 2.05 at 550 nm wavelength. The broad peaks in Raman spectra indicated the polycrystalline nature of the thin film. It was also observed that with the annealing temperature the intensity of the Raman peaks increased. From these results, it was proved that annealing significantly improved the crystallinity, microstructural, surface morphological and optical features of the barium titanate thin film which made it suitable as potential sensors in biomedical applications as it is cost-effective, lead-free and environment friendly material.*

Keywords: *Atomic Force Microscopy, Annealing, $BaTiO_3$ Thin film, Fourier Transform Infrared Spectroscopy, Kubelka-Munk, Optical Bandgap, Raman spectroscopy, Scanning Electron Microscopy, Tauc-plot, UV-Visible spectroscopy, X-ray Diffraction*

1. INTRODUCTION

Over the last decade, barium titanate ($BaTiO_3$) has materialized as a promising contender for a wide sort of applications owing to its excellent piezoelectric, dielectric and ferroelectric properties. $BaTiO_3$ belongs to the class of perovskite structure with a Curie temperature of 120 °C [1]. It is a wide-ranging ferroelectric substance having a high dielectric constant at higher room temperature, low cost, high chemical, and mechanical stability, low dielectric loss, comprehensively utilized for the manufacturing of electronic peripherals, such as piezoelectric devices, (MLCs) multilayer capacitors, PTC (positive temperature coefficient) thermistors, as well as a range of optoelectronic devices [2]. A great concentration has been given on the production of crystalline barium titanate ferroelectric thin films, to utilize its ferroelectric activity, high dielectric constant as well as nonlinear optical properties for numerous active and passive electronic devices.

Significantly, a lot of consideration has been targeted on the manufacturing process of high-quality crystalline $BaTiO_3$ thin films to attain improved application flexibility in addition to consistency with existing silicon fabrication technology [3]. Various techniques such as sputtering (DC and RF), evaporation (thermal, laser, two-boat, ash), metal-organic deposition, reactively partially ionized beam deposition, and metal-organic chemical vapor deposition (MOCVD) have being utilized for the deposition of $BaTiO_3$ thin films [4].

In this work, $BaTiO_3$ thin film is deposited using the simplest deposition technique, i.e., Electron Beam Evaporation (or e-beam evaporation). This is a dominant and economical PVD (Physical Vapor Deposition) technique that enables the user to vaporize materials which are strenuous to process by means of usual resistive thermal

[DOI: 10.22068/ijmse.1879]

evaporation method. There is an advantage of the e-beam evaporation technique that it enables the immediate energy transfer through the electron beam to the target substance to be evaporated making it ideally suited for high melting point metals. Few of these materials are high temperature materials for example gold, or ceramics like silicon dioxide, many other materials which are available in the powdered form. e-beam PVD process produces higher density films owing to its larger deposition rates which leads to improved adhesion with the substrate. This technique is superior to other PVD methods as it has higher material utilization efficiency and much cheaper. In the e-beam PVD process there is a lower level of contamination as it heats merely the target surface and not the whole crucible. As the energy is directed onto the target instead on the whole processing chamber, there is very less probability of substrate destruction due to high process temperature. These numerous benefits are the main motivation of using e-beam PVD technique for the investigation of the various significant properties of barium titanate thin film for nanoelectronic device applications [4-6].

The main aim of this work is to analyze the influence of annealing on the surface morphological, optical and microstructural properties of polycrystalline $BaTiO_3$ thin film for nanoelectronic and optoelectronic device applications. Different characterization methods are used for the investigation of these properties. The film is deposited over p-type Si < 100 > substrate using e-beam evaporation physical vapor deposition technique. To achieve the improved crystalline structure of the thin film, annealing is done using a conventional high-temperature tube furnace.

2. EXPERIMENTAL PROCEDURE

2.1. $BaTiO_3$ Thin Film Deposition

The $BaTiO_3$ thin film is grown onto p-type Si < 100 > substrate resistivity: 1—10 Ωcm and boron doping concentration:(7×10^{15} cm^{-3}) using the e-beam physical vapor deposition technique. For the deposition of $BaTiO_3$ thin film, first, the pellets of the 1 gm of 99% pure Barium Titanate (IV) powder with the particle size < 3 μm and density of 6.08 g/mL at 25 °C (lit.) (obtained from Sigma-Aldrich Chemical Pvt. Limited, India), are prepared using cylindrical steel die of 13 mm diameter [7]. Initially, die is kept in highly viscous mobile oil so that it can be prevented from rusting. After the extraction of the die from the oil, it is first degreased using acetone. The Hydrophobic stearic acid solution is applied on the inner surface of the die to avoid the adhesion of the powder before the granules are put into the die. The granules are first crushed into a mortar pestle to convert it into a smooth powder and then placed into the die, and the piston is slowly inserted into the cylinder. The die is pressed with a pressure of 5 bar using the hydraulic press and the pressure is maintained for 1.40 minutes. Ahead of loading the samples upon the sample holder, the cleaning of Si wafer is done by acetone solution to remove dust particle, organic substances and then the sample is treated with HF dip for 5 min (a solution of 1: 9, 10% Hydrofluoric acid and 90% Water) to remove the native silicon-dioxide from the silicon wafer. Since it acts quickly, one needs to only expose the wafer for a short time ("dip"). The $BaTiO_3$ pellets are then loaded into the crucible to serve as the target material for deposition. For the generation of e-beam, the electron beam vacuum coating unit (Model BC-300 from Hind High Vacuum Bengaluru, India) is operated at 5 kV, drawing a current of 30 mA respectively. Before the actual deposition, all these process parameters are optimized to achieve high-quality thin film. The vacuum for the deposition process is generated at 8×10^6 mbar pressure at room temperature. The substrate to target distance is kept at 18 cm which generates the focused electron beam of 3 cm diameter.

2.2. Annealing Procedure

After the deposition, the three different samples are then annealed at 400 °C, 600 °C, and 800 °C respectively, by means of high-temperature tube furnace (LTF 14/450) at the heating rate of 5 °C/min. with the dwell time of 30 minutes, 22 minutes and 15 minutes respectively, to attain a better crystalline thin film. In this furnace, silicon carbide rod is used as the heating element. It has a high response rate as the heating element radiates heat directly onto the tube. For achieving maximum thermal efficiency and stability low thermal mass insulation is used throughout the worktube of the furnace.

[DOI: 10.22068/ijmse.1879]

2.3. Characterization

The structural analysis is carried out using an Atomic Force Microscope (Multimode-8 Scanning Probe Microscope from Bruker Corporation, USA), in the tapping mode. The crystallographic study is done using X-ray Diffractometer (PANalytical X'Pert - PRO) utilizing Cu X-ray diffractometer operated at 45 kV and 45 mA rating with $Cu - K\alpha$ radiation (λ = 1.54060Å) at the scan rate of 0.02° at 12° min^{-1} in the 2θ range from 20° to 70°. The surface morphological properties of the deposited film are examined using Field Emission Scanning Electron Microscope (Nova Nano FE-SEM 450) operated in high vacuum mode at 15 kV using Through Lens Detector (TLD). The UV-Vis spectroscopy is accomplished using a UV-Visible spectrophotometer (Lambda 750 model from PerkinElmer) with 60 mm diameter integrating sphere.

The Raman spectral bands are identified using confocal micro Raman Spectrometer (STR 500) with 532 nm excitation laser, 12.5 mW laser power, 45second exposure, 20× objective lens and a 600G mm grating.

The FTIR spectroscopy is performed using (Spectrum two from PerkinElmer) for obtaining a plot between transmittance (%T) versus wavenumber (cm^{-1}).

3. RESULTS AND DISCUSSION

3.1. Structural Analysis

The crystalline behavior of the barium titanate thin film is investigated using XRD. The XRD patterns of $BaTiO_3$ thin film annealed at three different temperatures, 400 ℃, 600 ℃ and 800 ℃ respectively are shown in Fig. 1. The peak around 2θ ≈ 24° is associated with the p-type < 100 > Si substrate. The nature of the film is found to be

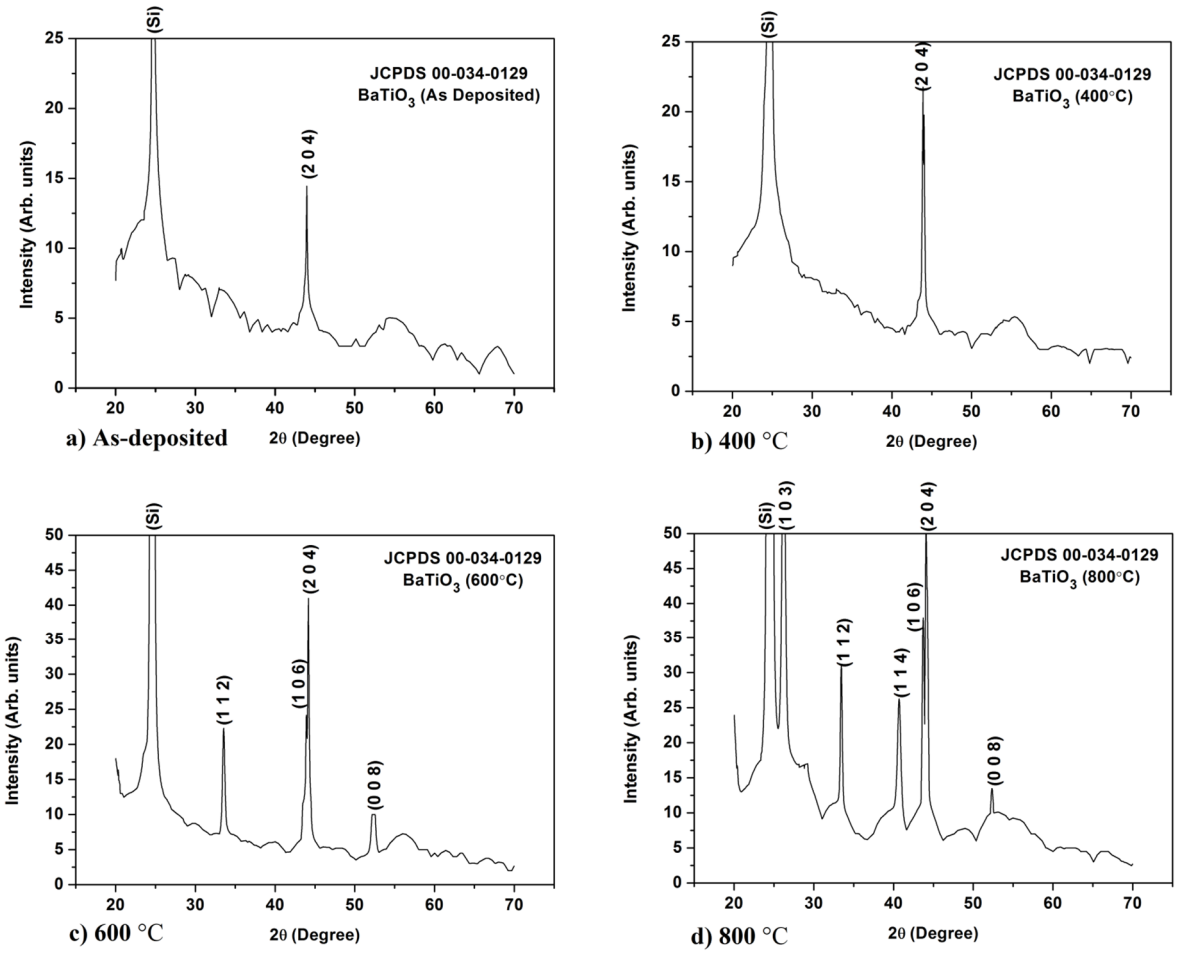

Fig. 1. XRD spectra of $BaTiO_3$ thin film at (a) As-deposited, (b) 400 ℃, (c) 600 ℃ and (d) 800 ℃ annealing temperatures

[DOI: 10.22068/ijmse.1879]

polycrystalline with a dominating diffraction peak at (204) crystallographic orientation. Some additional low-intensity peaks with (103), (112), (114), (106), (008), orientation are also observed. The grain size for (204) crystallographic orientation is calculated as 28.407 nm, 30.87 nm, 32.503 nm and 37.89 nm for as-deposited, 400 °C, 600 °C and 800 °C respectively, using Debye Scherrer's formula [8–12]

$$D = \frac{0.94\lambda}{\beta Cos\theta} \quad (1)$$

where λ, β and θ are the x-ray wavelength, the FWHM of the diffraction peak and the diffraction angle respectively.

A comparison of the measured peak positions with standard JCPDS card no.00-034-0129 suggests that all of the $BaTiO_3$ samples are crystalline. The XRD pattern of the samples confirms the hexagonal structure with space group (194) P63/mmc. There is no significant impurity phase in the sample. As it exhibits the centrosymmetric structure hence, it can be used as a piezoelectric material. The lattice parameters for the hexagonal structure are calculated as $a = b = 5.72652$ Å and $c = 13.96043$ Å (α = β = 90°; γ = 120°) with c/a ratio as 2.4378 using Hull-Davey chart as in Eq. (2) [13].

$$\frac{1}{d^2} = \frac{4}{3}\left(\frac{h^2 + hk + k^2}{a^2}\right) + \frac{l^2}{c^2} \quad (2)$$

where d is the particle spacing. These lattice constants and c/a ratio is in good agreement with the standard values a = b = 5.725 Å, c = 13.967 Å and c/a ratio as 2.44 obtained from the JCPDS card no. 00-034-0129. The lattice strain (ξ) is calculated as 1.27×10^{-3}, 1.22×10^{-3}, 1.111×10^{-3} and 9.553×10^{-4} for as-deposited, 400 °C, 600 °C and 800 °C respectively using the formula [8] in Eq (3):

$$\xi = \frac{\beta Cos\theta}{4} \quad (3)$$

During the layer formation, mechanical stress and strains are introduced by its subsequent heat treatment the dislocations are introduced which can be analytically measured by Eq. (4). The defect density or the dislocation density provides significant information about the crystal structure of the deposited thin film which can be described as the length of dislocations per unit volume and can be calculated as $1.239 \times 10^{-3} nm^{-2}$, $1.049 \times 10^{-3} nm^{-2}$, $9.465 \times 10^{-4} nm^{-2}$ and $6.965 \times 10^{-4} nm^{-2}$ for as-deposited, 400 °C, 600 °C and 800 °C respectively [8].

$$Dislocation\ Density = \frac{1}{D^2} \quad (4)$$

The peaks in the XRD spectrum possess high intensity with an increment in the grain size and the decrement in the FWHM, defect density and the strain with the increasing annealing temperature which improves the crystallinity and leads to the better quality of the thin film.

Fig. 2 depicts the $10 \times 10\ \mu m^2$ 3-D AFM images for the as-deposited, 400 °C, 600 °C and 800 °C respectively, each viewed at the scale of 2 µm. From these images, it can be analyzed that the RMS value of roughness increases from 31.5 nm, 33 nm, 50.6 nm & 52.8 nm for as-deposited, 400 °C, 600 °C and 800 °C respectively due to the enhancement in the grain size and the formation of agglomerates. The behaviour observed of the thin film is the same as reported in the previous work [14–19].

3.2. Surface Morphological Analysis

Fig. 3 (a) to (d) depicts the FESEM image of $BaTiO_3$ thin film at 50K× magnification and each viewed at the scale of 2 µm to explain the surface morphological changes with annealing temperature for as-deposited, 400 °C, 600 °C and 800 °C respectively. It has been observed that the grown film is uniform and homogeneous. Fig. 3(e) presents the cross-sectional view of the barium titanate film which proves the thickness of the deposited thin film to be around 210 nm. The measurement scale for all the SEM images are same and mentioned at the end of Fig. 3 (e). From the FESEM images, it can be visualized that the particle size gets increased with the annealing temperature and grain size varying in the range from 36 nm - 62 nm, making it suitable for nano-electronic device applications [16-17, 20].

3.3. Analysis of optical properties

The UV-Visible spectrophotometer with an integrating sphere of 60 mm diameter is attached for reflectance measurement which is used for the determination of optical bandgap. The optical reflectance of the $BaTiO_3$ thin film has been recorded from 200 nm to 800 nm range. The optical bandgap is analyzed using the Kubelka-Munk (K-M or F(R)) approach [21], which is based on the Eqs. from (5-8).

$$F(R_{ef}) = \frac{\left(1 - R_{ef}\right)^2}{2R_{ef}} \quad (5)$$

[DOI: 10.22068/ijmse.1879]

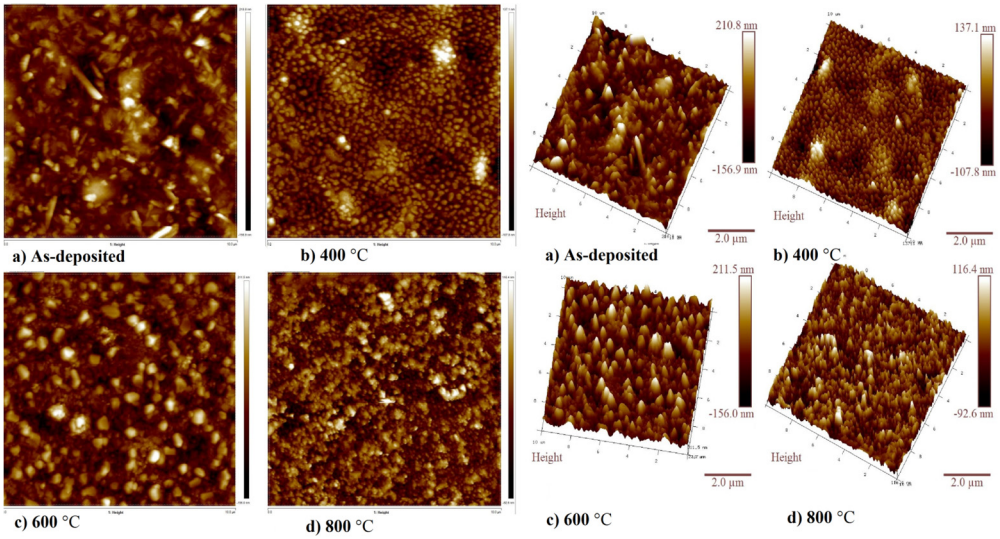

Fig. 2. 2-D and 3-D AFM images of $BaTiO_3$ thin film at (a) As-deposited, (b) 400 ℃, (c) 600 ℃ and (d) 800 ℃ annealing temperatures

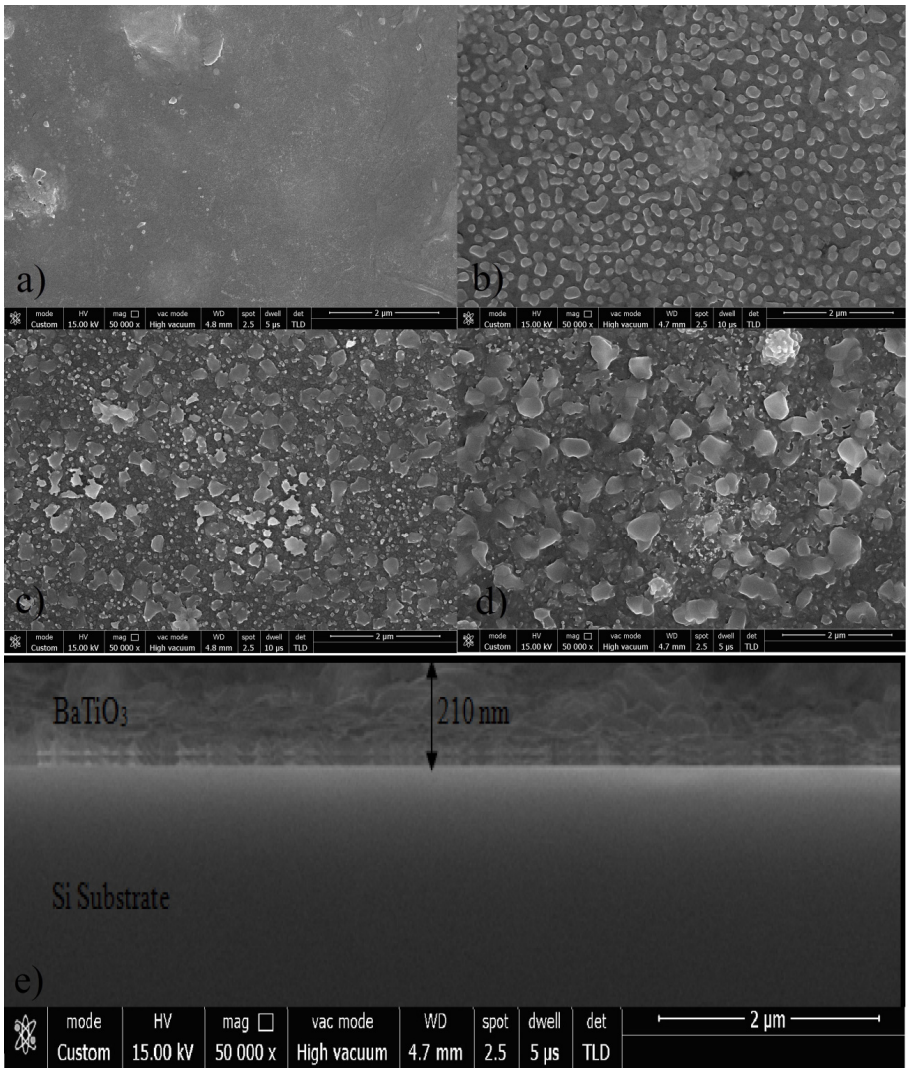

Fig. 3. FESEM images of BaTiO3 thin film at (a) As-deposited, (b) 400 ℃, (c) 600 ℃ and (d) 800 ℃ annealing temperatures and e) Cross-sectional image.

[DOI: 10.22068/ijmse.1879]

where $F(R_{ef})$ is proportional to the extinction coefficient (α), R_{ef} is the reflectance.

The photon energy (E) is calculated using the Brus formula as given by Eq. (6) [22].

$$E = h\nu = \frac{1240}{\lambda}\ (eV) \tag{6}$$

where h is the Planck's constant in eVs, λ is the wavelength in nm.

The $F(R_{ef})$ function is then multiplied with $h\nu$ to obtain the modified Kubelka-Munk function $(F(R_{ef})h\nu)$ and the bandgap E_g is calculated using Eq. (7-8) [21].

$$\alpha h\nu \approx B\left(h\nu - E_g\right)^n \tag{7}$$

The Eq. (7) can also be written as

$$F(R_{ef})h\nu \approx B(h\nu - E_g)^n \tag{8}$$

where B is the absorption constant, n represents the nature of band transition ($n = 1/2$ for the direct allowed transition; $n = 3/2$ for the indirect allowed transition) as reported in the literature.

To graphically analyze the bandgap from the reflectance data $n = 1/2$ is substituted in Eq. (8). A graph between modified K-M function $(F(Ref)h\nu)^2$ versus $h\nu$ is plotted. This plot is known as the Tauc plot [21–26] and is shown in Fig. 4. The bandgap E_g for the $BaTiO_3$ thin film from the tauc plot is calculated as 3.93, 3.9, 3.877 and 3.87 eV for as-deposited, 400 ℃, 600 ℃ and 800 ℃ respectively, which is in accordance with the reported values [23, 27-28]. This trend of decrement of bandgap with the increase in annealing temperature is also justified by Varshni's empirical expression [29] given by Eq (9).

$$E_g[T] = E_g[0] - \frac{\alpha T^2}{T + \beta} \tag{9}$$

where $E_g[T]$ is the energy bandgap at temperature T, $E_g[0]$ is the bandgap at the 0 °K, and α and β are constants.

The effect of annealing on different parameters of $BaTiO_3$ thin film is summarized in Table 1.

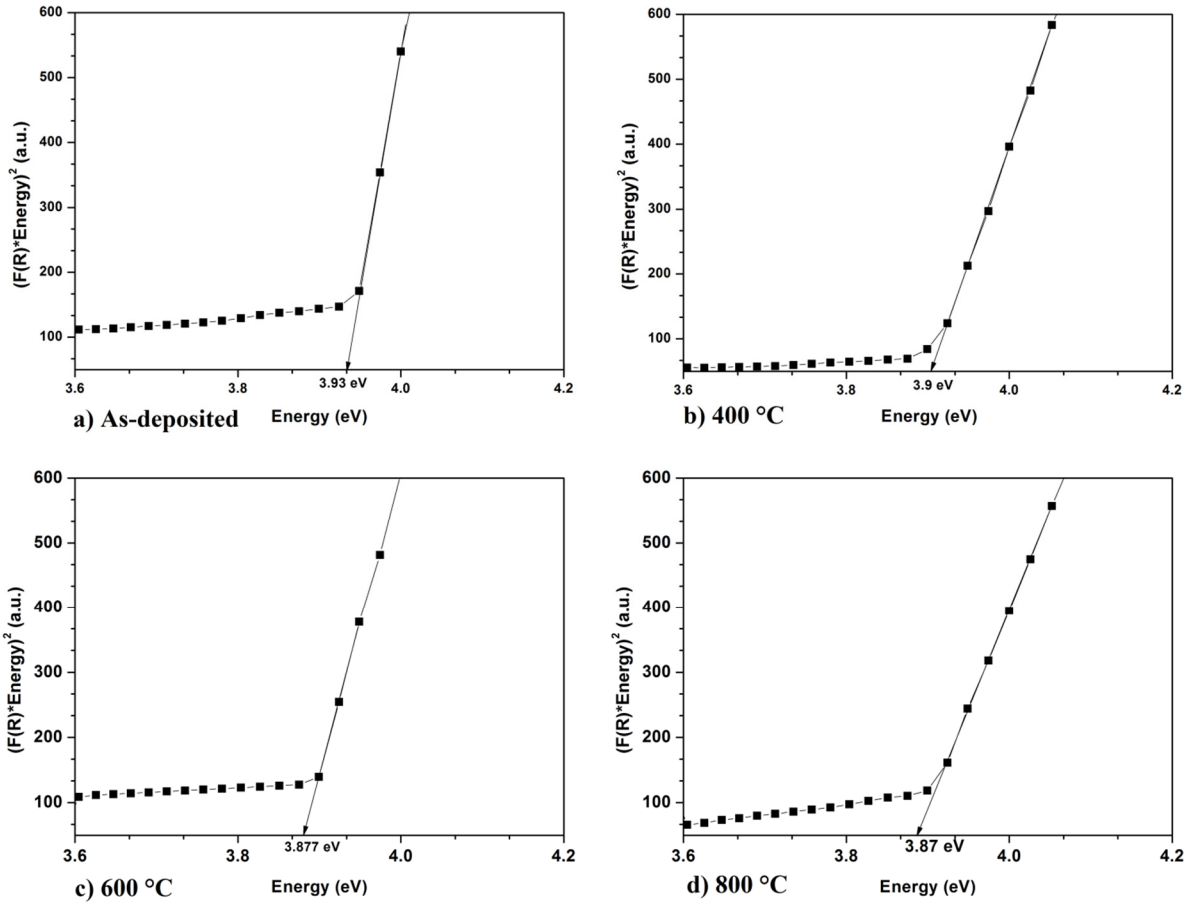

Fig. 4. Tauc plot of $BaTiO_3$ thin film at (a) As-deposited, (b) 400 ℃, (c) 600 ℃ and (d) 800 ℃ annealing temperatures

[DOI: 10.22068/ijmse.1879]

Table 1. The effect of annealing on different parameters of $BaTiO_3$ thin film

Annealing Temperature (°C)	Grain Size (D) (nm)	Defect Density (nm^{-2})	Strain (ξ)	Roughness (nm)	Bandgap (eV)
As-deposited	28.407	1.239×10^{-3}	1.27×10^{-3}	31.5	3.93
400 °C	30.87	1.049×10^{-3}	1.22×10^{-3}	33	3.9
600 °C	32.503	9.465×10^{-4}	1.111×10^{-3}	50.6	3.877
800 °C	37.89	6.965×10^{-4}	9.553×10^{-4}	52.8	3.87

The electro-optic (EO) response is determined by computing the refractive indices (n(λ)) of the $BaTiO_3$ thin film. For this the refractive indices are computed at each wavelength from the peaks and valleys of the interference oscillations and the measured reflectance. The plot of the refractive indices at each wavelength for the as-deposited, 400 °C, 600 °C and 800 °C annealed $BaTiO_3$ thin film is shown in Fig. 5. For polycrystalline $BaTiO_3$ thin film the refractive index varies from 2.2 to 1.98 from 400 to 500 nm and it is 2.05 at 550 nm wavelength. The curve shows nearly flat response beyond 550 nm wavelength and it is also noticed that there is slight decrement in the refractive index in accordance with the annealing temperature [4, 36].

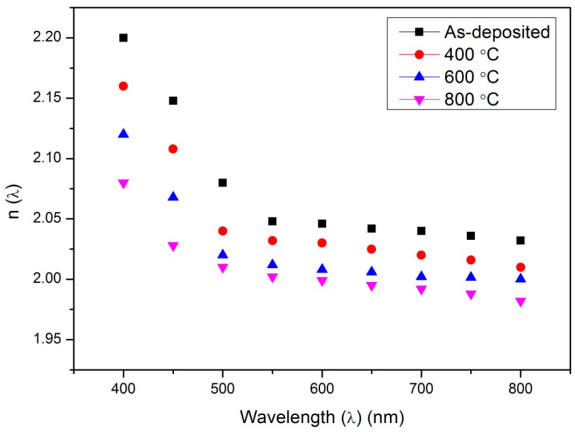

Fig. 5. Refractive index (n(λ)) versus wavelength (λ) for (a) as-deposited, (b) 400 ℃, (c) 600 ℃ and (d) 800 ℃ annealing temperature

The comparison among all the optical properties with the available literature is summarised in Table 2.

The Raman spectrum of $BaTiO_3$ thin film for various annealing temperatures is depicted in Fig. 6 (a, b). The Raman spectra are recorded from 200 nm to 800 nm. In the Raman spectra, peak around 302 cm^{-1} is associated with Si. The remaining peaks are associated with $BaTiO_3$ out of which the peak at 247 cm^{-1} is associated to the A1 (Transverse Optic (TO)) mode, the peak about 304 cm^{-1} designates the E((Longitudinal Optic) (LO) +TO), B1) mode. The peaks around 422, 437 cm^{-1} are associated with E2(high) phonon mode and the peak at 519 cm^{-1} is designated to E(TO) mode. These modes are associated with the crystallinity of $BaTiO_3$ film and are due to the displacement of Ti^{4+} ions because of annealing at high temperatures [31]. From Fig. 6 (a, b), it can be visualized that the strength of the Raman bands increases along with the heating temperature which again justifies that the as-deposited film annealed at 800 °C can be used for optoelectronic applications. The broad peaks indicate the poly-crystalline feature of the thin film [26, 30].

In Fig. 7 the transmittance (%T) versus wavenumber (cm^{-1}) of $BaTiO_3$ thin film at distinct annealing temperatures is demonstrated from 4000 - 450 cm^{-1}. The dints or minima in the graph indicate the absorption maxima analogous to the typical groups and molecules. The transmittance peaks marked in Fig. 7 designate their bond strength. The N─H, ≡C─H, Hydrogen-bonded O─H, H─C─H Asymmetric & Symmetric stretching modes of vibration occurs at the higher wavenumbers in the different functional groups including alkynes, amides, carboxylic acids, and alkanes respectively, in the range from 3500-2400 cm^{-1}. The peaks in the range from 2300-2200 cm^{-1} denotes the occurrence of C≡N stretching mode. The tip in the range from 1755-1650 cm^{-1} results from the C=O stretching mode of vibration due to the presence of esters. The peaks that originate between 1675-1600 cm^{-1} and 1550-1450 cm^{-1} signifies the existence of C-C=C Symmetric stretching mode and N─H bend relates to the alkenes and secondary-amines respectively. There is an occurrence of N=O bend from the range of 1400-1300 cm^{-1} associated with the nitro

[DOI: 10.22068/ijmse.1879]

Table 2. Comparison of optical properties of the proposed work with the available literature

S. No.	Parameter	This Work			Reference			
		Film Orientation	Range	Deposition Method	Ref. No.	Film Orientation	Range	Deposition Method
1	Optical Bandgap (eV)	z-axis	3.93 to 3.87 for as-deposited, 400 °C, 600 °C and 800 °C annealed film	e-beam PVD	[8]	NR	2.97 - 2.91 for 500 °C to 900 °C annealing temperature	$BaTiO_3$ powders prepared by wet chemical method
					[23]	NR	3.88 to 3.47 500 °C to 900 °C annealing temperature	$BaTiO_3$ Nanoparticles
					[24]	NR	3.14 to 3.19 for 299K to 465K annealing temperature	Conventional solid-state reaction route using $BaCO_3$ (99.99%) and TiO_2 (99.99%)
2	Refractive index n(λ)	z-axis	2.2 to 1.98 from 400 to 500 nm and 2.05 at 550 nm, Flat response after 550 nm	e-beam PVD	[4]	NR	2.2 to 1.98 from 400 to 500 nm and 2.05 at 550 nm	Metallo-organic solution deposition technique
					[36]	NR	2.4 to 2.2, flat after 550 nm	Plused laser deposition

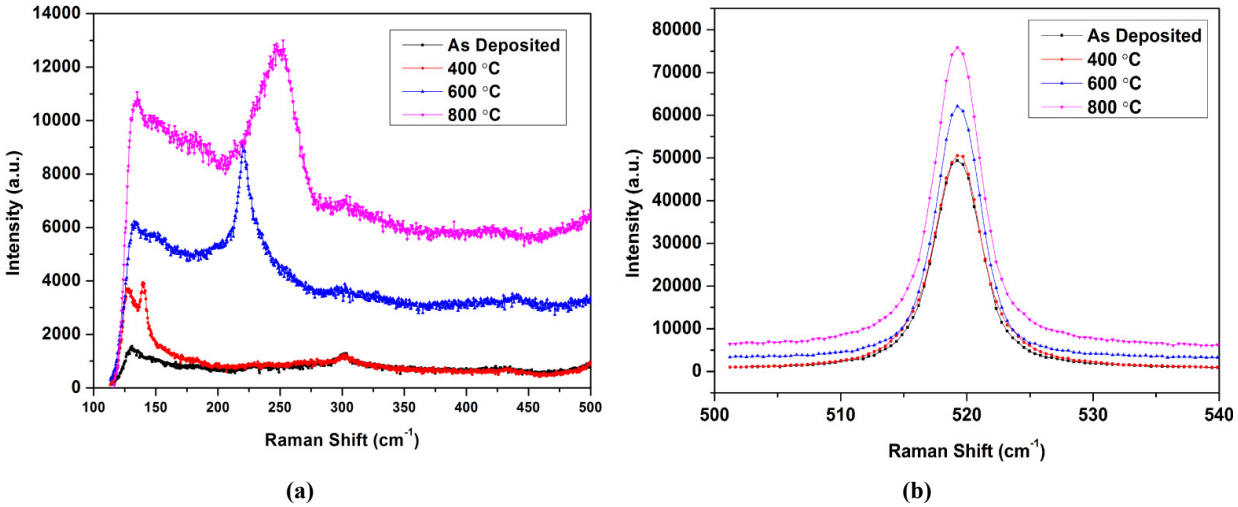

Fig. 6. The Raman Spectra of $BaTiO_3$ thin film at different annealing temperatures. (a) Raman Shift from 100 to 500 cm^{-1} and (b) Raman Shift from 501 to 550 cm^{-1}

[DOI: 10.22068/ijmse.1879]

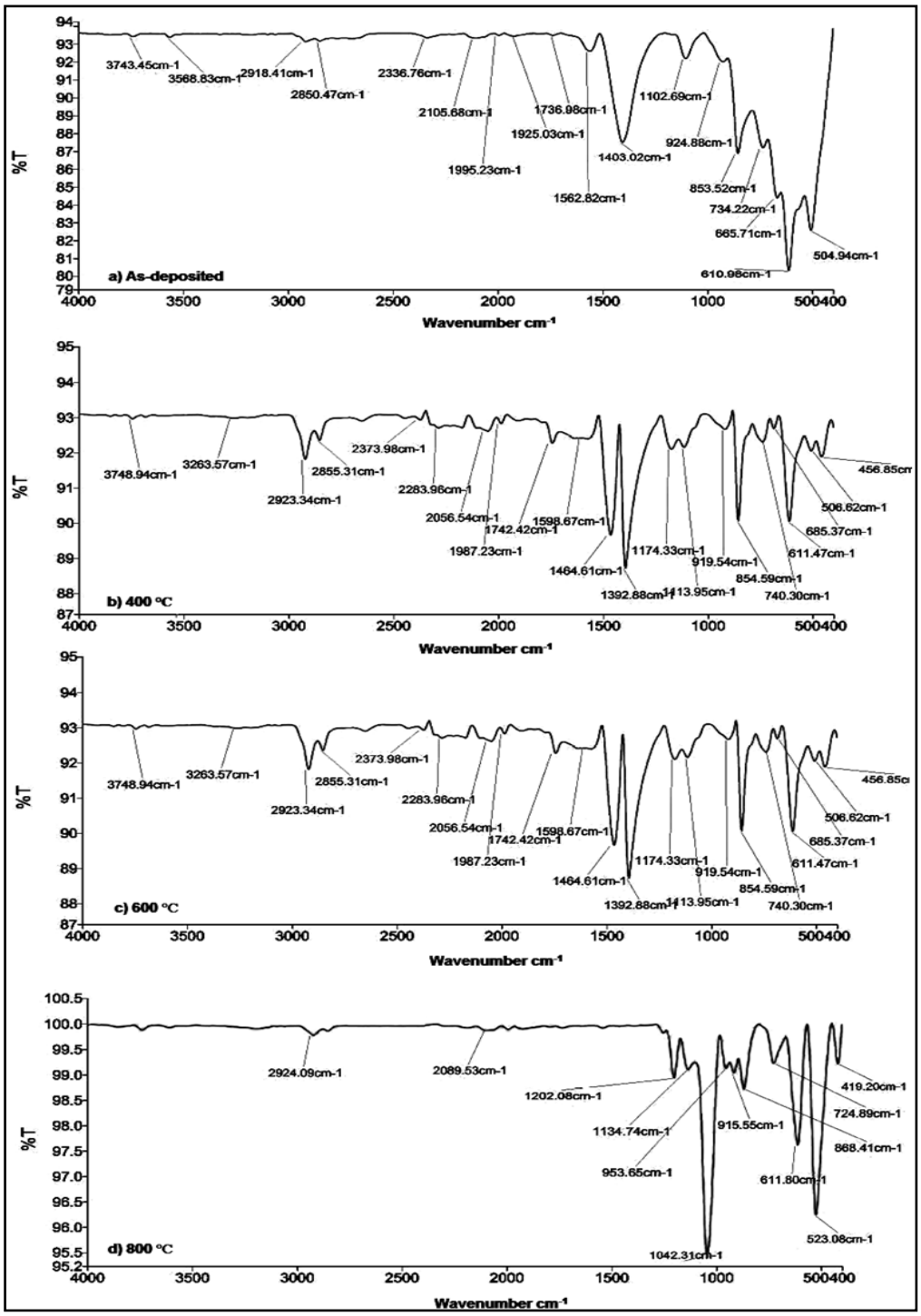

Fig. 7. FTIR spectrum of $BaTiO_3$ thin film at (a) As-deposited, (b) 400 ℃, (c) 600 ℃ and (d) 800 ℃ annealing temperatures

groups. The absorption peaks between 1300 and 1000 cm^{-1} denote the C-O vibration stretching mode because of ethers. The peaks occur at the lower wavenumbers are due to the existence of methylene and alkyne functional groups [31–35].

4. CONCLUSIONS

The effect of annealing on the surface morphology, microstructural and optical features of polycrystalline barium titanate thin film,

[DOI: 10.22068/ijmse.1879]

deposited on p-type Si <100 > substrate using e-beam physical vapour deposition technique was reported in this paper. The enhancement in the grain size from 28.407 to 37.89 nm was analogous to the increment in annealing temperature, with a decrement in dislocation density, strain and FWHM. This made the grown film suitable for nanoelectronic applications. Due to annealing, the RMS value of roughness got increased from 31.5 to 52.8 nm which also added to the grown film property. The optical band gap reduced from 3.93 to 3.87 eV for the as-deposited, 400□, 600□ and 800□ respectively with the increased annealing temperature. Reduction in the bandgap made the annealed film suitable for optoelectronic applications and as sensors for health monitoring purposes. For polycrystalline $BaTiO_3$ thin film the refractive index varied from 2.2 to 1.98 from 400 to 500 nm and it was 2.05 at 550 nm wavelength. A significant improvement in crystalline, structural, morphological and optical features of the grown thin film was achieved by annealing.

5. ACKNOWLEDGMENT

The authors wish to gratefully acknowledge DRDO, New Delhi for providing financial support to this project. The authors would also like to thank Materials Research Center (MRC) at MNIT, Jaipur for providing all the facilities required for the experimentation work.

6. REFERENCES

[1] W. Hsiao-Lin, "Structure and dielectric properties of perovskite - Barium titanate ($BaTiO_3$)", Chemical and Materials Engineering Dept., San Jose State University, 2002. http://citeseerx.ist.psu.edu/viewdoc/download?doi=10.1.1.520.7708&rep=rep1&type=pdf.

[2] M. Vijatovic Petrovic, J. Bobic, B. Stojanovic, "History and Challenges of Barium Titanate: Part I", Science of Sintering, 2008, 40, 155-165. https://doi.org/10.2298/SOS0802155V.

[3] M. Vijatovic Petrovic, J. Bobic, B. Stojanovic, "History and Challenges of Barium Titanate: Part II", Science of Sintering, 2008, 40, 235-244. https://doi.org/10.2298/SOS0803235V.

[4] P.C. Joshi, S.B. Desu, "Structural, electrical, and optical studies on rapid thermally processed ferroelectric $BaTiO_3$ thin films prepared by metallo-organic solution deposition technique", Thin Solid Films, 2008, 300, 289-294. https://doi.org/10.1016/S0040-6090 (96)09468-0.

[5] C. Feldman, "Formation of Thin Films of $BaTiO_3$ by Evaporation", Review of Scientific Instruments, 1955, 26 (5), http://dx.doi.org/10.1063/1.1771326.

[6] M.J Madou, "Fundamentals of Microfabrication: the science of miniaturization", CRC Press, 2002.

[7] B. Mojtaba, G. Magdalena, F. Stachowicz and T. Trzepiecinski, Acta Mechanica, "Synthesis of Barium Titanate Piezoelectric Ceramics for Multilayer Actuators (MLAs)", Automatica, 2017, 11, 275-279. https:// doi.org / 10.1515 / ama-2017 -0042.

[8] R. Sengodan, B. Chandar Shekar and S.Sathish, "Structure, surface morphology and and optical properties of $BaTiO_3$ powders prepared by wet chemical method", Indian Journal of Pure and Applied Physics, 2014, 52, 839-845. http://op.niscair.res.in/index.php/IJPAP/article/view/3257/398.

[9] S. S. Kumbhar, M. A. Mahadik, P.K. Chougule, V. S. Mohite, Y. M. Hunge, K.Y. Rajpure, A.V. Moholkar and C.H. Bhosale, "Structural and electrical properties of barium titanate ($BaTiO_3$) thin films obtained by spray pyrolysis method", Materials Science-Poland, 2015 , 33, 852-861. https://doi.org/10.1515/msp-2015-0107.

[10] J. H. T. Evans, "An X.Ray Diffraction Study of Barium Titanate", Technical Report (1953), 58, 1-35, https://pdfs.semanticscholar.org/b2cf/1ce3293d6ca0d286f184631dff367b8b4d37.pdf.

[11] R. K. Singh, S. Sanodia, N. Jain, and R.Kumar, "Effect of Mechanical Milling on Barium Titanate ($BaTiO_3$) Perovskite", American Institute of Physics, 2018, 130017-1-130017-4, https://doi.org/10.1063/1.5033161.

[12] R. Ashiri, "Analysis and Characterization of Phase Evolution of Nanosized $BaTiO_3$ Powder Synthesized Through a Chemically Modified Sol-Gel Process", Metall and

[DOI: 10.22068/ijmse.1879]

Mat. Trans A, 2012, 43, 4414 - 4426. https://doi.org/10.1007/s11661-012-1242-1.

[13] A.W. Hull and W.P. Davey, "Graphical Determination of Hexagonal and Tetragonal Crystal Structures from X-Ray Data", Phys. Rev., 1921, 17, 549-570. https://doi.org/10.1103/PhysRev.17.549.

[14] V. TorresHeredia, J. MuñozSaldaña, Real de Juriquilla, F. J. Espinoza Beltrán, A. Márquez Herrera, A. Zapata Navarro, "Microstructural Characterization of BaTiO3 Thin Films Prepared by RF-Magnetron Sputtering Using Sintered Targets from High Energy Ball Milled Powders", The AZo Journals of Materials Online, 2005, 3117, 1-13, https://doi.org /10.2240/azojomo0159.

[15] K. M. Yeung, C. L. Mak, K. H. Wong and G. K. H. Pang, "Preparation of $BaTiO_3$ Thin Films of Micrometer Range Thickness by Pulsed Laser Deposition on (001) $LaAlO_3$ Substrates", Japanese Journal of Applied Physics, 2004, 43, 6292 - 6296. doi.org / 10.1143 / JJAP.43.6292.

A. Solanki, J. Shrivastava, S. Upadhyaya, S. Choudhary, V. Sharma, P. Sharma, P. Kumar, P. Kumar, S. Ehrman, V. R. Satsangi, R. Shrivastava and S. Dass, "Modified structural, morphological and photoelectrochemical properties of 120 MeV Ag^{9+} ion irradiated $BaTiO_3$ thin films", Current Applied Physics, (2013), 13, 344 – 350. https://doi.org/10.1016 /j.cap.2012.08.005.

B. K. S. Riaz, S. Shamaila, S. Naseem, "Barium Titanate Films for Electronic Applications: Structural and Dielectric Properties", Surface Review and Letters, 2008, 15, 237-244. https://doi.org/10.1142 /S0218625X08011305.

[16] R. Ashiri, A. Nemati and M. S. Ghamsari, "Crack-free nanostructured $BaTiO_3$ thin films prepared by sol–gel dip-coating technique", Ceramics International, 2014, 40, 8613-8619. https://doi.org/10.1016 /j.ceramint.2014.01.078.

[17] R. Ashiri, "A Mechanistic Study of Nanoscale Structure Development, Phase Transition, Morphology Evolution, and Growth of Ultrathin Barium Titanate Nanostructured Films", Metallurgical and Materials Transactions A, 2014, 45, 4138-4154. https://doi.org/10.1007/s11661-014-2352-8.

[18] R. Ashiri, A. Nemati, M. S. Ghamsari and M. M. Dastgahi, "Nanothickness films, nanostructured films, and nanocrystals of barium titanate obtained directly by a newly developed sol–gel synthesis pathway", Journal of Materials Science:Materials in Electronics, 2014, 25, 5345-5355. https://doi.org/10.1007/s10854-014-2312-5.

[19] R. Lopez and R. Gomez, "Band-gap energy estimation from diffuse reflectance measurements on sol–gel and commercial TiO_2: a comparative study", J Sol-Gel Sci Technol., (2012), 61, 1-7. https://doi.org/10.1007/s10971-011-2582-9.

[20] J. Mayandi, S. Mahalakshmi, V. Ragavendran, "Optical and structural studies of $BaTiO_3$ and $SrTiO_3$", J. Nanosci. Nanotechnol., 2014, 2, 735-735.

[21] E A. Mgbemeje, S. M. Akhtar, Y. O. Bong and C. D. Kue, "Influence of Annealing Temperatures on the Structural, Morphological, Crystalline and Optical properties of $BaTiO_3$ and $SrTiO_3$ Nanoparticles", J Material Sci Eng., 2016, 5, 1-6. https://doi.org/10.4172/2169-0022.1000277.

[22] V. Mishra, A. Sagdeo, K. Warshi, H. M. Rai, S. K. Saxena, R. Kumar and P.R. Sagdeo, "Metastable behavior of Urbach tail states in $BaTiO_3$ across phase transition", Condensed Matter: Strongly correlated Electrons, 2016 https://arxiv.org /abs/1612.06756v1.

[23] P.E. Agbo, "Effect of thermal annealing on optical and band gap of chemically deposited TiO_2/Fe_2O_3 core/shell oxide thin films". J. Adv Appl. Sci Res., 2011, 2, 393-399.

[24] K. I. Osman, "Synthesis and characterization of $BaTiO_3$ ferroelectric material. Metallurgical Engineering", Faculty of Engineering, 2011. https://inis.iaea.org/collection/NCLCollectionStore/_Public/44/079/44079115.pdf.

[25] R. Ashiri, Ali Nemati, M. Sasani Ghamsari and H. Aadelkhani, "Characterization of optical properties of amorphous $BaTiO_3$ nanothin films", Journal of Non-Crystalline Solids, 2009, 355, 2480-2484.

[DOI: 10.22068/ijmse.1879]

https://doi.org/10.1016/j.jnoncrysol.2009.08.030.

[26] R. Ashiri, "Analysis and Characterization of Relationships Between the Processing and Optical Responses of Amorphous $BaTiO_3$ Nanothin Films Obtained by an Improved Wet Chemical Process", Metallurgical and Materials Transactions B, 2014, 45, 1472–1483. https://doi.org /10.1007/s11663-014-0057-4.

[27] Y.P. Varshni, "Temperature dependence of the energy gap in semiconductors", Physica, 1967, 34, 149-154. https://doi.org /10.1016/0031-8914 (67) 90062-6.

[28] M. B. Smith, K. Page, T. Siegrist, P. L. Redmond, E. C. Walter, R. S., Louis E. Brus and M. L. Steigerwald, "Crystal Structure and the Paraelectric-to-Ferroelectric Phase Transition of Nanoscale $BaTiO_3$", Journal of the American Chemical Society, (2008), 130, 6955-6963. https://doi.org/10.1021/ja0758436.

[29] Z. Lazarevic, N. Romcevic, M. Vijatovic, N. Paunovic, M. Romcevic, B. Stojanovic and Z. Dohcevic-Mitrovic, "Characterization of Barium Titanate Ceramic Powders by Raman Spectroscopy", ACTA PHYSICA POLONICA A, 2009, 115 808-810. http://przyrbwn.icm.edu.pl/APP/PDF/115/a115z412.pdf.

[30] L.R. Prado, N.S. de Resende, R.S. Silva, S.M.S. Egues, G.R. Salazar-Banda, "Influence of the synthesis method on the preparation of barium titanate nanoparticles", Chemical Engineering and Processing: Process Intensification, 2016, 103, 12-20. https://doi.org/10.1016/j.cep.2015.09.011.

[31] S. G. Prasad, A. De and U. De, "Structural and Optical Investigations of Radiation Damage in Transparent PET Polymer Films", International Journal of Spectroscopy, 2011, 810936 1-7, http://dx.doi.org/10.1155/2011/810936.

[32] M. C. de Andrade, G. N. Carneiro, E. L. Moreira, J. C. Araujo and V.C.A. Moraes, "Synthesis and Characterization of Barium Titanate by Solid-State Reaction", Materials Science Forum. (2014), 802, 285-290. doi.org/10.4028 /www.scientific.net/MSF.802.285.

[33] K. M. Jarabana, A. Mishra and S. Bisen, "Structural and Optical properties of poly-crystalline $BaTiO_3$ and $SrTiO_3$ prepared via solid state route", Journal of Physics: Conference Series. 2016, 755, 012020. doi.org/ 10.1088/1742-6596/755/1/012020.

[34] K.T.Al-Rasoul, Issam M. Ibrahim, Qusay A. Hussein, "Structural and optical properties of $BaTiO_3$ thin films prepared by pulsed laser deposition", Iraqi Journal of Physics, 2012, 10, 41-44.

[DOI: 10.22068/ijmse.1879]